Journal of Thermal Analysis and Calorimetry, Vol. 94 (2008) 1, 263–270

SYNTHESIS AND KINETIC ANALYSIS OF ISOTHERMAL AND NON-ISOTHERMAL DECOMPOSITION OF AMMONIUM DINITRAMIDE PRILLS

G. Santhosh and Ang How Ghee*

Energetic Materials Research Centre, Nanyang Technological University, 50 Nanyang Avenue, Singapore 639 798

Ammonium dinitramide (ADN) prills were prepared by emulsion crystallization and characterized by optical microscopic, thermogravimetric (TG) and differential scanning calorimetric (DSC) techniques. The isothermal and non-isothermal decomposition kinetics of ADN prills were studied by TG. The differential isoconversional method of Friedman (FR) and integral isoconversional method of Vyazovkin were used to investigate the dependence of activation energy (E_a) with conversion (α) and the results were compared with literature data. The dependence of activation energy was also derived from isothermal data. A strong dependence of E_a with α is observed for the ADN prills. All the methods showed an initial increase in E_a up to α=~0.2 and later decreases over the rest of conversion. The apparent E_a values of FR method are higher than that of Vyazovkin method up to α=~0.45. The calculated mean E_a values by FR, Vyazovkin and standard isoconversional method for α between 0.05 and 0.95 were 211.0, 203.9 and 156.9 kJ mol^{-1}, respectively.

Keywords: *activation energy, ammonium dinitramide, emulsion crystallization, model-free kinetics, thermal decomposition*

Introduction

Over the past few decades, there has been a rapidly increasing interest and demand for the development and use of new energetic materials for a variety of space and military applications [1, 2]. A promising oxidizer from the class of dinitramide i.e. ADN whose structure shown in Fig. 1 is becoming more attractive as potential replacements for ammonium perchlorate (AP) and ammonium nitrate (AN) because of its predictable burn rate, residue-less combustion, absence of halogen and carbon atoms and high performance [3–5]. Studies on its synthesis, combustion and propellant formulations have been published [6–9]. Theoretical calculations indicate that solid propellant formulations of ADN in various energetic binder systems will outperform the conventional AP/HTPB formulations in terms of specific impulse (I_{sp}). To date, considerable emphasis has been placed on studying the decomposition kinetics of ADN and several works devoted to these have been published [10–16]. The results from a detailed analysis of the mechanism and decomposition of ADN can be used to derive its combustion characteristics. Despite being regarded as a high performance oxidizer, ADN resulting from the synthesis has undesirable crystal shape and poor morphology, which prevents its use in propellant formulations and is often necessary to tailor the crystal shape by proper crystallization/prilling methods [17].

Two different technologies were developed for the formation of spherical ADN particles. The prilling tower method as described by Highsmith *et al*. whereby the molten ADN is sprayed through a nozzle on the top of a huge glass column having hot and cold zones and allow it to fall under gravity on a counter current flow of cold inert gas [18, 19]. The molten grains of ADN on contact with the cold gas solidify and the same is collected at the bottom of the prilling tower. In the second method as described by Teipel *et al*. ADN is melted in hot paraffin oil and stirred thoroughly until the molten ADN is uniformly dispersed [20, 21]. The molten ADN grains are then subsequently cooled to ambient temperature and the formed prills are isolated from the oil and washed with a solvent, the process is known as emulsion or melt crystallization. The spherical ADN particles obtained from the above methods are generally referred to as ADN prills. The prills under our present study were obtained from an emulsion crystallization process. The ADN prills are reported to possess higher thermal stability and are less sensitive than the crystalline ADN resulting from the synthesis [22, 23] and the use of bimodal mixtures of ADN prills of varying particle

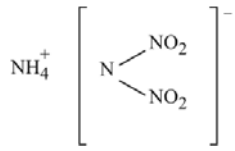

Fig. 1 Chemical structure of ADN

* Author for correspondence: gsanthosh@ntu.edu.sg

1388–6150/$20.00

Akadémiai Kiadó, Budapest, Hungary
Springer, Dordrecht, The Netherlands

sizes in a propellant composition is expected to offer a higher solid loading and a high theoretical maximum density (TMD).

The solid-state reactions which involve a change in extensive property such as mass (TG) and enthalpy (DSC) have attracted wide interest as their kinetics can be studied by thermoanalytical methods [24]. The kinetics of such reactions is normally studied under isothermal and/or non-isothermal conditions. The thermal analysis of energetic materials is one of the prime areas which is being explored in great detail. A traditional model fitting approach using a single curve method has been found to involve various curve-fitting techniques and gives only a set of kinetic parameters (i.e. kinetic triplets namely $\ln A$, E_a, $f(\alpha)$ or $g(\alpha)$). Reliable predictions on the decomposition of a substance cannot be made with this approach over the range of experimental temperatures. The kinetic triplets from the model-fitting technique from non-isothermal experiments are highly uncertain and cannot be compared with the kinetic triplets obtained from isothermal experiments. The International Confederation of Thermal Analysis and Calorimetry (ICTAC) project emphasizes the use of multi-heating rate and isoconversional methods for the kinetic computations [25]. The use of model-free methods is a trustworthy way of obtaining reliable and consistent kinetic information and increasingly being used for energetic materials [26–28], polymers [29–31] and other materials [32]. The kinetic analyses of the thermal decomposition of ADN by model fitting and model-free isoconversional analysis were reported in the literature [33–37]. However the thermal decomposition kinetics of ADN prills has not been studied so far. A thorough investigation on the thermal decomposition of ADN prills will provide better understanding of its physical and chemical characteristics that affect the solid propellants during the storage and use.

In this paper, we describe a laboratory scale process for producing ADN prills and the detailed kinetic analyses of decomposition data of the prills. The kinetic parameters and the apparent activation energy on conversion evaluated by model-free methods are presented.

Experimental

Materials

The ADN prills were prepared in the laboratory by emulsion crystallization and their melting points were determined by DSC. The samples were characterized by spectral and thermal methods. Paraffin oil (J.T. Baker) was used as received.

Methods

TG experiments were carried out using a Shimadzu TGA-50 thermogravimetric analyzer. Non-isothermal runs were performed at constant heating rates of 2, 3 and 6°C min^{-1}. Isothermal runs were performed at 125, 135, 145 and 150°C. Samples were placed in aluminium pans and heated in a flowing nitrogen (50 mL min^{-1}) atmosphere. A constant sample mass of 3.5–4 and 4.5–5 mg of samples were used for the non-isothermal and isothermal experiments, respectively. DTG curves were generated by smoothed numerical derivatives of TG curves.

DSC measurements were performed using a TA instruments DSC 2010 differential scanning calorimeter under a nitrogen flow of 50 mL min^{-1}. A constant sample mass of 2 to 2.5 mg is used for all the experiments. Samples were taken in aluminium pans.

An Olympus BX-51 microscope was used for the optical measurements of ADN prills.

The data analysis and kinetic calculations from the TG measurements were done either by using Microsoft® EXCEL, Microcal ORIGIN® or Mathworks MATLAB® softwares.

Results and discussion

Emulsion crystallization

The process involves the melting of ADN in paraffin oil maintained above the melting point of ADN i.e. 92°C. The experimental setup is shown in Fig. 2. Paraffin oil is taken in a flat glass vessel (GV) and placed on a magnetic stirrer hotplate (HP). The temperature of the paraffin oil is controlled by a thermocouple (TC) immersed in the oil. The stirring of the oil and molten ADN is achieved by placing a rectangular flat

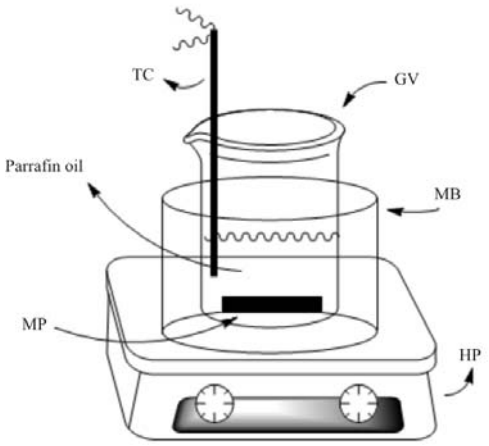

Fig. 2 Experimental setup for the emulsion crystallization of ADN TC – thermocouple, GV – glass vessel, MB – metallic bath, MP – magnetic pellet, HP – hotplate

magnetic pellet (MP). The whole assembly is placed in a metallic bath (MB) which allows to quickly cool the glass assembly with a coolant. Once the required temperature of the paraffin oil i.e. 92–93°C is reached, the recrystallized ADN is slowly introduced into the paraffin oil under constant stirring.

ADN melts in paraffin oil and the stirring of the oil aids in forming molten grains. After the complete formation of the molten grains, the whole assembly is slowly cooled to ambient temperature whereby the molten ADN crystallizes to hard spherical grains. The hard spherical grains were removed from the paraffin oil by filtration and then washed few times with methylene chloride and dried under vacuum.

Characterization of ADN prills

The ADN prills were then analysed by DSC. As seen from Fig. 3, the melting point of ADN prills is 91.89°C which is slightly lower than the recrystallized ADN which is melting at 92.44°C. The lowering

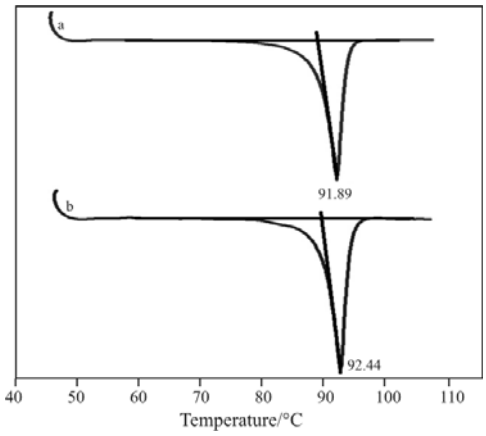

Fig. 3 DSC Melting traces of ADN: a – prills and b – recrystallized

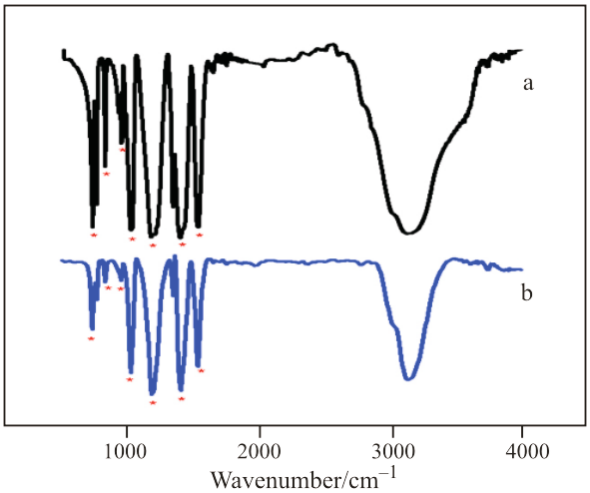

Fig. 4 Overlay of IR spectrum of ADN: a – prills and b – recrystallized

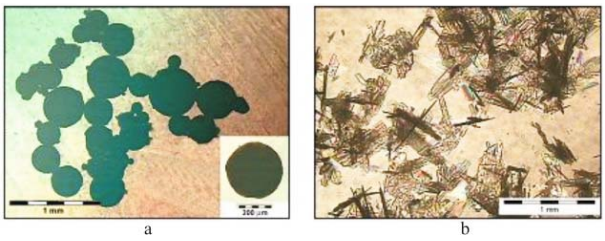

Fig. 5 Optical microscopic images of ADN: a – prills and b – recrystallized

of the melting point can be attributed either to the thermal stability of ADN at its melting point or the presence of trace amounts of the medium (paraffin oil) during the emulsion crystallization process.

Comparison of the infrared (IR) spectra of ADN (prills and recrystallized) (Fig. 4) showed that both are identical in shape and all the characteristic vibrations were retained. Each characteristic vibrations of ADN are marked with an asterisk in Fig. 4. The IR frequencies of ADN can be found elsewhere [38].

The recrystallized ADN and the prills are subjected to optical microscopic analysis. The optical microscopic images of recrystallized and emulsion crystallized ADN prills are shown in Fig. 5.

It can be seen that the recrystallized ADN have irregular needle shaped crystals, while the emulsion crystallized ADN prills are spherical. The particle size of ADN prills as measured from optical microscopy is in the range of 100 to 300 μm.

Thermal analysis

The thermal analyses of ADN prills were carried out by TG to study the phenomenological aspects of ADN. Figure 6 shows the TG-DTG curves of ADN prills at a heating rate of 2°C min^{-1}; similar curves were obtained for all other heating rates.

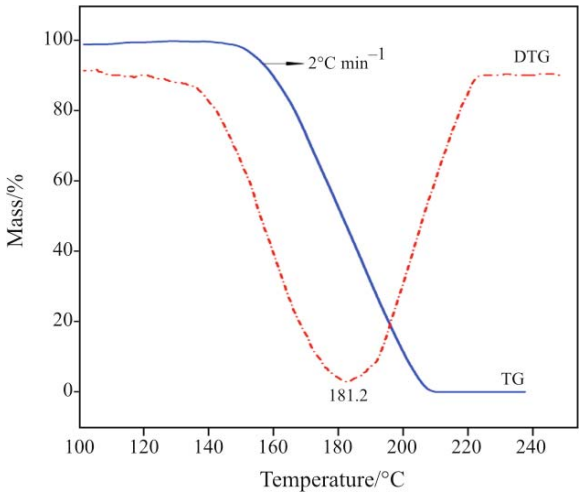

Fig. 6 TG and DTG curves of ADN prills in N_2 atmosphere

The TG measurements showed that ADN prills undergo single stage decomposition with a 100% mass loss in the temperature range of 145 to 230°C, as it gets converted to volatile decomposition products. The well-defined DTG curve with a peak maximum at T~181°C also indicates that it decomposes in a single step. The literature reports indicate that the decomposition of ADN is controlled by the experimental conditions and different mechanisms were postulated by many authors [11, 37, 39]. A generalized decomposition mechanism shown in Scheme 1 suggests that the decomposition of ADN produces various oxides of nitrogen where the formation of ammonia and dinitramidic acid [$HN(NO_2)_2$] dominate in the first step (below 100°C) followed by further decomposition of the latter and AN formed by the recombination of NH_3 and HNO_3 at higher temperature (above 100°C).

$$\left.\begin{aligned} &NH_4N(NO_2)_2 \rightarrow \\ &\rightarrow NH_3 + HN(NO_2)_2 \\ &HN(NO_2)_2 \rightarrow \\ &\rightarrow HNO_3 + N_2O \end{aligned}\right\} \text{low temperature}$$

$$\left.\begin{aligned} &NH_3 + HNO_3 \rightarrow \\ &\rightarrow NH_4NO_3 \\ &NH_4NO_3 \rightarrow \\ &\rightarrow N_2O + 2H_2O \\ &HN(NO_2)_2 \rightarrow \\ &\rightarrow NO_2^+ + HNNO_2^- \end{aligned}\right\} \text{high temperature}$$

Scheme 1 Thermal decomposition pathways of ADN

Apart from the decomposition fragments shown in Scheme 1, many other products were also evolved in varying ratios depending on the experimental conditions. The thermal decomposition of ADN reported by Brill *et al*. showed the presence of NH_3, N_2O, NO_2, H_2O, NO, N_2, HNO_3 and NH_4NO_3 [39].

The values of initial temperature (T_0), peak temperature (T_p) (from DTG), final temperature (T_f) and the extent of reaction at maximum rate α_{max} at various heating rates are given in Table 1. The extent of conversion (α) is calculated from Eq. (1).

$$\alpha = \frac{W_i - W_a}{W_i - W_f} \quad (1)$$

where, W_a, W_i and W_f are the actual, initial and final sample mass, respectively.

It is evident from Table 1 that the characteristic decomposition temperatures of all the samples showed a shift as the heating rate is increased and the values of α_{max} also showed a similar trend. The variation of α with temperature (T) during the thermal decomposition of ADN prills at various heating rates is shown in Fig. 7.

Table 1 Characteristic temperatures of decomposition for ADN prills from TG

Heating rate/ °C min^{-1}	T_0/°C	T_p/°C	T_f/°C	α_{max}
2	147.6	181.2	207.6	0.499
3	148.6	183.0	211.9	0.502
6	152.3	188.0	230.2	0.511

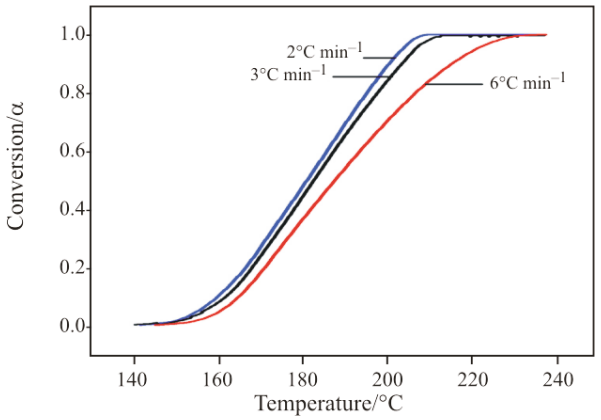

Fig. 7 Variation of conversion (α) with temperature at various heating rates during the thermal decomposition of ADN prills

It is seen from Fig. 7, that the run at 2°C min^{-1} covers a temperature range of 150–205°C, where as the run at 6°C min^{-1} covers about 150–230°C.

Isothermal experiments were conducted at 125, 135, 145 and 150°C on the ADN prills. The thermogravimetric data showing the extent of conversion of ADN prills during isothermal decomposition are shown in Fig. 8. Taking into consideration the slow decomposition of ADN above 125°C, isothermal experiments were carefully performed and no conversion is observed within the time gap when the samples were heated from ambient to the experimental isothermal temperature.

As seen from Fig. 8, the extent of conversion is low at 125°C and is high at higher temperatures. The extent of conversion is quite rapid at 145 and 150°C, which can be attributed to the exothermic decomposition of ADN prills.

Kinetic analysis

Dynamic and isothermal TG techniques are promising tools to reveal the kinetics and mechanisms of the physical and chemical processes occur during the thermal decomposition of ADN. The kinetic analyses have been carried out by model-free approaches. By the application of model-free kinetics one can obtain

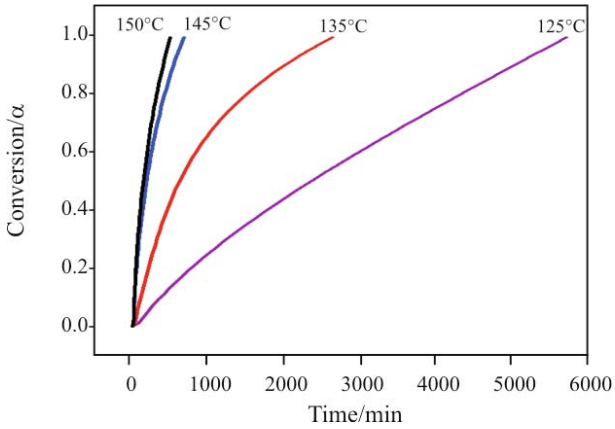

Fig. 8 Variation of conversion (α) with time during the isothermal decomposition of ADN prills. The temperature (in°C) is indicated by each curve

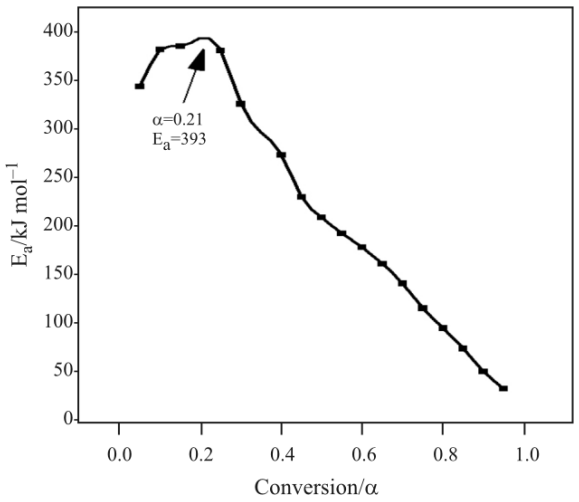

Fig. 9 Apparent activation energy (E_a) as a function of conversion (α) for the decomposition of ADN prills by FR method

reliable and consistent kinetic information about the overall process. The model-free kinetics assumes no particular model in deriving the activation energy. This approach follows all the conversion points from multiple experiments performed at various heating rates instead of a single experiment at a fixed heating rate. The basic equation of non-isothermal kinetic analysis (TG, DSC, etc.) is based on the rate equation shown in Eq. (2).

$$\beta\frac{d\alpha}{dT}=f(\alpha)A\exp\left(-\frac{E_a}{RT}\right) \qquad (2)$$

where α is the degree of conversion, T is the temperature, β is the linear heating rate, A is the pre-exponential factor, E_a is the activation energy, $f(\alpha)$ is the differential function of conversion and R is the gas constant. Starting from Eq. (2) various methods were developed to evaluate the kinetic triplets. However the use of isoconversional methods permit the estimation of E_a without the prior knowledge of the analytical form of the conversion function $f(\alpha)$. The non-isothermal data from multiple heating rates on the decomposition of ADN prills were analyzed by Friedman and Vyazovkin methods.

Friedman's method

The method suggested by Friedman [40] shown in Eq. (3) is obtained by simple rearrangement of Eq. (2). It permits estimation of the activation energy without the knowledge of the form of $f(\alpha)$.

$$\ln\left(\frac{d\alpha}{dt}\right)_{\alpha,i}=\ln[A_\alpha f(\alpha)]-\frac{E_\alpha}{RT_{\alpha,i}} \qquad (3)$$

where subscript i denotes different heating rates. This method requires numerical differentiation of the experimental α *vs*. T curves for each heating rate. For a constant α, the plots of ln(dα/dt) *vs*. $1/T$, at several heating rates, gives a straight line from whose slope the activation energy can be calculated.

The dependence of activation energy as a function of conversion by FR method is shown in Fig. 9. It shows that the apparent E_a is not constant and it increases from ~340 kJ mol^{-1} (α=0.05) to ~393 kJ mol^{-1} (α=0.2) and decreases further to ~35 kJ mol^{-1} (α=0.95). The mean activation energy for conversion (0.05≤α≤0.2) is 370.2 kJ mol^{-1} and for conversion (0.2<α≤0.95) is 176.9 kJ mol^{-1}. The activation energy profile obtained for the ADN prills indicates two distinct zones above and below conversion 0.2 which could be attributed to the two competing reaction pathways outlined in Scheme 1.

Vyazovkin's method for kinetic analysis

Model-free kinetics method of Vyazovkin was used to determine the apparent activation energy over conversion. The general assumption used in Vyazovkin's method is that the pathway is independent of heating rate. For a set of experiments carried out at different heating rates, the activation energy $E_{a\alpha}$ can be determined at any particular desired value of α by finding the value of $E_{a\alpha}$ for which the function Ω is minimum as shown in Eq. (4)

$$\Omega=\sum_{i=1}^{n}\sum_{j\neq i}^{n}\frac{\beta_j I(E_{a\alpha},T_{\alpha i})}{\beta_i I(E_{a\alpha},T_{\alpha j})} \qquad (4)$$

The indexes i and j in Eq. (4) denote different heating rates, n is the total number of heating rates and I is the temperature integral. The temperature integral I is given by Eq. (5)

$$I(E_{a\alpha},T_{\alpha i})=p(x)=\int_0^{T_{\alpha i}}\exp\left(\frac{-E_{a\alpha}}{RT}\right)dT \qquad (5)$$

The temperature integral in Eq. (5) can be evaluated by various popular approximation methods and also by direct numerical integration methods.

The temperature integral $p(x)$, where $x=E_a/RT$ can be approximated by a popular Senum and Yang non-linear approximation [41]. In our studies fourth (four terms) rational approximation of Senum and Yang as shown in Eq. (6) is used.

$$p(x)=\frac{e^{-x}}{x}\cdot\frac{(x^3+18x^2+86x+96)}{(x^4+20x^3+120x^2+240x+120)} \quad (6)$$

The minimization of Eq. (4) is done in MATLAB using the medium scale quasi-Newton method with a mixed quadratic and cubic line search procedure. The in-built function 'fminunc' is applied for the optimization.

The plot of dependence of activation energy with conversion is shown in Fig. 10.

It can be seen from the Fig. 10 that the E_a increases to a maximum of 308 kJ mol^{-1} around 28% conversion, thereafter it decreases over the rest of the conversion. The trend and shape of the apparent activation energy computed by Vyazovkin method is similar to that of FR method. The mean activation energy for conversion ($0.05\leq\alpha\leq0.2$) is 268.1 kJ mol^{-1} and for conversion ($0.2<\alpha\leq0.95$) is 180.9 kJ mol^{-1}.

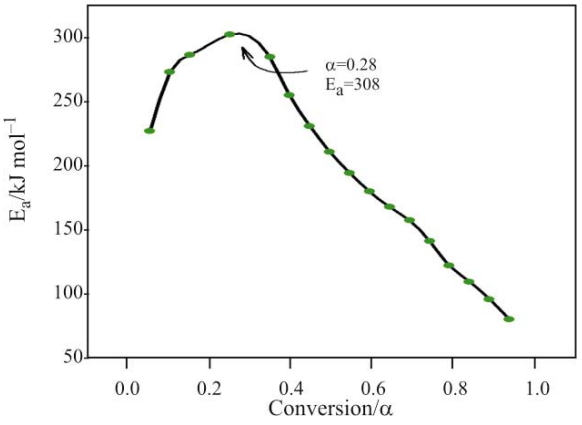

Fig. 10 Dependence of activation energy on conversion for the non-isothermal decomposition of ADN prills using Vyazovkin method

Comparison of results from FR and Vyazovkin method

The calculated values of the apparent activation energies by FR and Vyazovkin methods for ADN prills are presented together with the literature data for ADN in Fig. 11. The data for ADN was taken from [33]. The dependence of E_a with α is consistent with the reported trend observed for neat crystalline ADN by Vyazovkin *et al*. [33, 37].

It can be seen from Fig. 11 that the isoconversional methods have showed a maximum activation energy

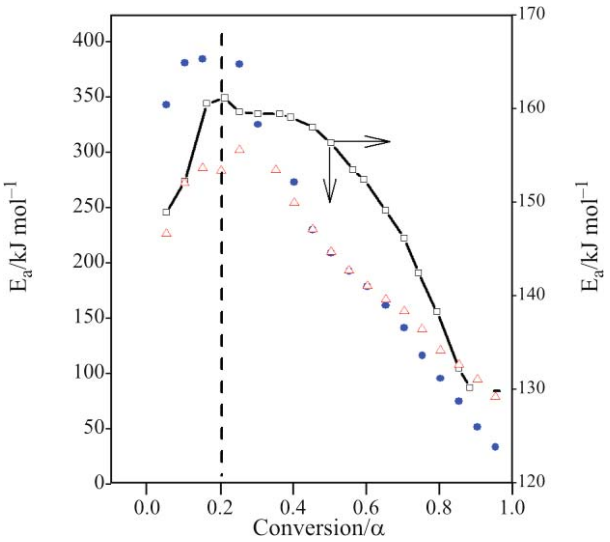

Fig. 11 Dependence of E_a on α for FR (ADN prills: ● – β=2, 3 and 6°C min^{-1}); Vyazovkin's (ADN prills: △ – β=2, 3 and 6°C min^{-1}) and literature data (ADN: □ – β=1.5, 4 and 5.5°C min^{-1})

at conversion $\alpha=\sim0.2$ (dotted lines). At conversions above 0.2, the activation energy decreases very fast. For conversions upto 0.45, the activation energies obtained by FR method are higher than that of Vyazovkin method and at conversions above 0.65, the E_a values by Vyazovkin method are higher. The susceptibility of the Friedman's method to errors arising from experimental noise and also the assumption of constant E_a over the conversion in Vyazovkin's method can be contributed to the observed difference in the E_a profiles. A comparison of our results on the dependence of activation energy for ADN prills with that of the results by Vyazovkin *et al*. shows that the E_a values vary significantly with conversion and the E_a values for the prills are much higher than that of the values obtained by Vyazovkin *et al*. for ADN. The E_a profile for the literature data at conversions above 0.2 deviates from that of ADN prills. The higher activation energy for the ADN prills clearly shows that it possesses higher thermal stability.

Isoconversional method for isothermal data

The dependence of activation energy (E_a) with conversion (α) is derived using standard isoconversional method [34] for the thermal decomposition of ADN prills under isothermal conditions. This is derived from the isothermal rate law as shown in Eq. (7)

$$g(\alpha)=Ae^{\frac{-E_a}{RT}}t \quad (7)$$

where t is the time and $g(\alpha)$ is the reaction model. Taking logarithm of Eq. (7) one can get Eq. (8).

$$\ln g(\alpha) = \ln A - \frac{E_a}{RT} + \ln t \quad (8)$$

For each α, rearrangement of Eq. (8) gives Eq. (9).

$$-\ln t_\alpha = \ln\left[\frac{A}{g(\alpha)}\right] - \frac{E_{a\alpha}}{RT} \quad (9)$$

where t_α is the time at conversion α. Under isothermal conditions for each α, $E_{a\alpha}$ is calculated from the slope of the plot of $-\ln t_\alpha$ *vs.* $1/T$ regardless of the model. Equation (9) has been applied to the isothermal data for the decomposition of ADN prills (data from Fig. 8) which permits the determination of E_a as a function of α. The dependence of activation energy on conversion for the isothermal decomposition of ADN prills is shown in Fig. 12.

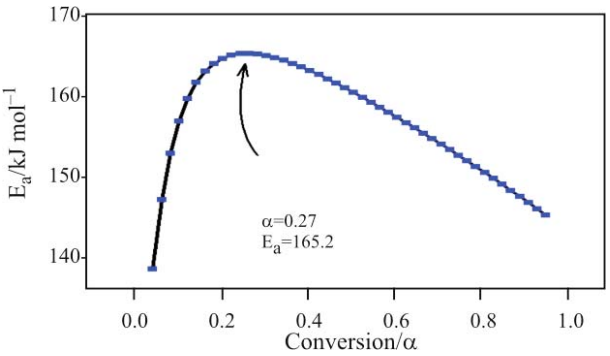

Fig. 12 Dependence of activation energy on conversion for the isothermal decomposition of ADN prills

It is seen that the E_a values bear a strong relationship to the degree of conversion. The activation energy rises from about 100 kJ mol^{-1} at low conversion to about 165 kJ mol^{-1} at α=0.27 and it subsequently decreases to 145 kJ mol^{-1} near the completion of the reaction. The mean activation energy for conversion ($0.05 \le \alpha \le 0.27$) is 151.9 kJ mol^{-1} and for conversion ($0.27 < \alpha \le 0.95$) is 156.3 kJ mol^{-1} which is lower than that of the values obtained by FR and Vyazovkin method. In the present study a comparison of the dependencies of E_a on α by non-isothermal and isothermal methods should not be made because the former covers a wide range of temperature (120 to 230°C) while the latter covers a narrow range of temperature (125 to 150°C).

Conclusions

ADN prills were prepared by emulsion crystallization and non-isothermal and isothermal kinetic investigations of the decomposition of ADN were carried out. Nonlinear isoconversional techniques were applied to evaluate the variation of E_a with α at various conversions for ADN prills. The dependence of E_a with α by all the methods is similar in shape and the apparent E_a values for conversion ($0.2 < \alpha \le 0.95$) are in the order of Vyazovkin >FR>standard isoconversional method. In the initial stages of decomposition ($0.05 \le \alpha \le 0.2$), the E_a value increases and in the latter stages ($0.2 < \alpha \le 0.95$) it decreases. A comparison of the results obtained indicates that the thermal stability of ADN prills was much higher than that of neat crystalline ADN.

References

1 J. C. Bottaro, Chem. Ind., (1996) 249.
2 S. Borman, Chem. Eng. News, (1994) 18.
3 A. Langlet, N. Wingborg and H. Ostmark, Challenges in Propellants and Combustion –100 Years After Nobel, K. K. Kuo, Ed., Begell House, New York 1997, p. 616.
4 M. L. Chan, A. Turner and L. Merwin,Challenges in Propellants and Combustion –100 Years After Nobel, K. K. Kuo, Ed., Begell House, New York 1997, p. 627.
5 J. C. Bottaro, P. E. Penwell and R. J. Schmitt, J. Am. Chem. Soc., 119 (1997) 9405.
6 S. Venkatachalam, G. Santhosh and K. N. Ninan, Prop. Expl. Pyro., 29 (2004) 178.
7 R. Yang, P. Thakre and V. Yang, Comb. Expl. Shock Waves, 41 (2005) 657.
8 C. J. Hinshaw, R. B. Wardle and T. K. Highsmith, PCT WO 9424073 A1, 1994.
9 C. J. Hinshaw, R. B. Wardle and T. K. Highsmith, US Patent 5498303, 1998.
10 M. J. Rossi, J. C. Bottaro and D. F. McMillen, Int. J. Chem. Kin., 25 (1993) 549.
11 J. C. Oxley, J. L. Smith, W. Zheng, R. Rogers and M. D. Coburn, J. Phys. Chem. A, 101 (1997) 5646.
12 A. S. Tompa, R. F. Boswell, P. Skahan and C. Gotzmer, J. Thermal. Anal., 49 (1997) 1161.
13 S. Vyazovkin and C. A. Wight, J. Phys. Chem. A, 101 (1997) 7217.
14 A. S. Tompa, Thermochim. Acta, 357–358 (2000) 177.
15 G. Santhosh, S. Venkatachalam, A. U. Francis, K. Krishnan, K. B. Catherine and K. N. Ninan, 33rd Int. Annu. Conf. ICT, 2002, p. 64-1.
16 G. Santhosh, S. Venkatachalam, K. Krishnan, K. B. Catherine and K. N. Ninan, 34th Int. Annu. Conf. ICT, 2003, p. 16-1.
17 P. Sjoberg, R. Wardle and T. Highsmith, Insensitive Munitions and Energetic Materials Technology Symposium, 2001, Vol. 1, p. 466.
18 T. K. Highsmith, C. S. McLeod, R. B. Wardle and R. Hendrickson, US Patent No. 6136115 and WO 99/01408, 1999.
19 T. K. Highsmith and H. E. Johnston, US Patent No. 6610157, 2003.
20 U. Teipel, T. Heintz and H. Krause, Prop. Expl. Pyro., 25 (2000) 81.
21 U. Teipel, Chem. Eng. Technol., 27 (2004) 751.
22 S. Karlsson and H. Ostmark, 11th Int. Det. Symp., 1998, p. 801.

23 N. Wingborg and M. van Zelst, Report No. FOA-R-00-01423-SE, 2000.
24 T. Ozawa, Thermochim. Acta, 355 (2000) 35.
25 M. E. Brown, M. Maciejewski, S. Vyazovkin, R. Nomen, J. Sempere, A. Burnham, J. Opfermann, R. Strey, H. L. Anderson, A. Kemmler, R. Keuleers, J. Janssens, H. O. Desseyn, Chao-Rui Li, T. B. Tang, B. Roduit, J. Malek and T. Mitsuhashi, Thermochim. Acta, 355 (2000) 125.
26 G. Singh and D. K. Pandey, J. Therm. Anal. Cal., 82 (2005) 353.
27 A. K. Sikder, J. Therm. Anal. Cal., 79 (2005) 631.
28 A. K. Burnham and L. N. Dinh, J. Therm. Anal. Cal., 89 (2007) 479.
29 S. Vyazovkin and N. Sbirrazzuoli, Macromol. Rapid. Commun., 27 (2006) 1515.
30 H. Polli, L. A. M. Pontes and A. S. Araujo, J. Therm. Anal. Cal., 79 (2005) 383.
31 A. K. Burnham and R. K. Weese, Thermochim. Acta, 426 (2005) 85.
32 A. Pratap, T. L. S. Rao, K. N. Lad and H. D. Dhurandhar, J. Therm. Anal. Cal., 89 (2007) 399.
33 S. Vyazovkin and C. A. Wight, Int. Rev. Phys. Chem., 17 (1998) 407.
34 S. Vyazovkin and C. A. Wight, Thermochim. Acta, 340–341 (1999) 53.
35 S. Vyazovkin and C. A. Wight, J. Phys. Chem. A, 101 (1997) 8279.
36 S. Vyazovkin and C. A. Wight, Annu. Rev. Phys. Chem., 48 (1997) 125.
37 S. Vyazovkin and C. A. Wight, J. Phys. Chem., 101 (1997) 5653
38 K. O. Christe, W. W. Wilson, M. A. Petrie, H. H. Michels, J. C. Bottaro and R. Gilardi, Inorg. Chem., 35 (1996) 5068.
39 T. B. Brill, P. J. Brush and D. G. Patil, Comb. Flame, 92 (1993) 178.
40 H. L. Friedman, J. Polym. Sci. Part C, 6 (1963) 183.
41 G. I. Senum and R. T. Yang, J. Thermal Anal., 11 (1977) 445.

Received: December 21, 2007
Accepted: April 16, 2008
OnlineFirst: August 15, 2008

DOI: 10.1007/s10973-007-8941-7